10-14-1998

Transport of ER Vesicles on Actin Filaments in Neurons by Myosin V

George M. Langford
Syracuse University

Joel S. Tabb
Dartmouth College

Bradley J. Molyneaux
Dartmouth College

Darien L. Cohen
Dartmouth College

Sergei A. Kuznetsov
Universität Rostock

Journal of Cell Science 111, 3221-3234 (1998)
Printed in Great Britain © The Company of Biologists Limited 1998
JCS7291

Transport of ER vesicles on actin filaments in neurons by myosin V

Joel S. Tabb[1,2,*], Bradley J. Molyneaux[1,2], Darien L. Cohen[1,2,‡], Sergei A. Kuznetsov[3] and George M. Langford[1,2,§]

[1]Department of Biological Sciences, Dartmouth College, Hanover, NH 03755-3576, USA
[2]Marine Biological Laboratory, Woods Hole, MA 02543, USA
[3]Tierphysiologie, Universität Rostock, D-18051 Rostock, Germany
*Present address: Department of Physiology, College of Veterinary Medicine, Cornell University, Ithaca, NY 14853, USA
‡Recovery Sciences, Genetech, Inc, 1 DNA Way, MS#3, South San Francisco, CA 94080-4990, USA
§Author for correspondence

Accepted 5 September; published on WWW 14 October 1998

SUMMARY

Axoplasmic organelles in the giant axon of the squid have been shown to move on both actin filaments and microtubules and to switch between actin filaments and microtubules during fast axonal transport. The objectives of this investigation were to identify the specific classes of axoplasmic organelles that move on actin filaments and the myosin motors involved. We developed a procedure to isolate endoplasmic reticulum (ER) from extruded axoplasm and to reconstitute its movement in vitro. The isolated ER vesicles moved on exogenous actin filaments adsorbed to coverslips in an ATP-dependent manner without the addition of soluble factors. Therefore myosin was tightly bound and not extracted during isolation. These vesicles were identified as smooth ER by use of an antibody to an ER-resident protein, ERcalcistorin/protein disulfide isomerase (EcaSt/PDI). Furthermore, an antibody to squid myosin V was used in immunogold EM studies to show that myosin V localized to these vesicles. The antibody was generated to a squid brain myosin (p196) that was classified as myosin V based on comparisons of amino acid sequences of tryptic peptides of this myosin with those of other known members of the myosin V family. Dual labeling with the squid myosin V antibody and a kinesin heavy chain antibody showed that the two motors colocalized on the same vesicles. Finally, antibody inhibition experiments were performed with two myosin V-specific antibodies to show that myosin V motor activity is required for transport of vesicles on actin filaments in axoplasm. One antibody was made to a peptide in the globular tail domain and the other to the globular head fragment of myosin V. Both antibodies inhibited vesicle transport on actin filaments by greater than 90% compared to controls. These studies provide the first direct evidence that ER vesicles are transported on actin filaments by myosin V. These data confirm the role of actin filaments in fast axonal transport and provide support for the dual filament model of vesicle transport.

Key words: Myosin V, ER transport, Squid giant axon, Organelle/vesicle movement, Actin filament, Axonal transport

INTRODUCTION

Video-enhanced contrast, light microscopy studies of motility in squid axoplasm provided the first direct evidence that organelles move on microtubules (Allen et al., 1985). Subsequent studies revealed that axoplasmic organelles also move on actin filaments during fast axonal transport (Kuznetsov et al., 1992). One of the outstanding questions regarding motility in axoplasm is the identity of the specific classes of organelles that move on actin filaments. Therefore we conducted a set of experiments designed to identify the organelles that move on actin filaments in the squid giant axon and to determine the myosin motor involved in their movement.

In previous studies, we showed that organelles in the giant axon of the squid switch between actin filaments and microtubules during movement (Kuznetsov et al., 1992). These observations provided the first evidence that both microtubules and actin filaments are required for fast axonal transport. The close interrelationship of the two cytoskeletal systems raised the interesting question of the specific role of each system (Atkinson et al., 1992). Our working hypothesis is that microtubules provide the tracks for movement over long distances while actin filaments provide the tracks for movement locally (Langford et al., 1994; Langford, 1995; Langford and Molyneaux, 1998). Long distance movement is defined as movement of vesicles from one location in the cell to another when the sites are physically separated. Local movement, on the other hand, is defined as: (a) movement of vesicles from a functional site to a closely adjacent microtubule domain in the cytoplasm, and (b) from a microtubule domain to the actin rich cortex at the plasma membrane or, in the case of neurons, to the actin network in the dendritic spines and axon terminals. This model of transport, referred to as the *dual filament model of transport* (Langford, 1995), is thought to be a general mechanism of transport of vesicles in cells and may

include transport of cytosolic components such as mRNA (Erdelyi et al., 1995; Haarer et al., 1994; Bobola et al., 1996; Long et al., 1997; Takizawa et al., 1997).

Axoplasmic organelles that move on actin filaments range in size from 50 nm (size of synaptic vesicles) to 1 μm (size of mitochondria). These organelles move at an average speed of 1 μm/second and can be observed to move over distances of several μm (Kuznetsov et al., 1992). Using the actin filament bundle in the acrosomal process of horseshoe crab sperm as a polarity marker, we showed that organelles moved toward the barbed ends of actin filaments (Langford et al., 1994). Therefore the actin-dependent organelle motors are barbed-end directed myosins, and are presumed to be members of one or more of the classes of unconventional myosins (Cheney and Mooseker, 1992; Mooseker and Cheney, 1995).

While many of the organelles that move in axons are free vesicles of various sizes, one class of organelle observed to move on actin filaments in the squid giant axon is a reticular network made of tubulovesicular elements. The tethered vesicles within these networks are able to move on actin filaments but movement is restricted to short excursions because the connecting membrane tubules limit the distance a given vesicle is able to travel (Kuznetsov et al., 1994). These tubulovesicular organelles resemble most closely smooth endoplasmic reticulum (Metuzals et al., 1997). Tubulovesicular organelles are known to be abundant in axons (Ellisman and Lindsey, 1983; Metuzals et al., 1983; Hodge and Adelman, 1980; Nakata et al., 1998) and have been shown to be transported primarily in the anterograde direction. For example, studies of axonal transport in the mouse saphenous nerves have shown that tubulovesicular organelles accumulate at the proximal side of a locally applied cold blockade (Tsukita and Ishikawa, 1980). Using morphological criteria, these tubulovesicular elements were described as smooth ER.

In this study, we devised a procedure to isolate the endoplasmic reticulum from the giant axon of the squid without fragmenting the complex into microsomes as occurs during homogenization. Using this method, we were able to visualize the complex morphology of this organelle at the light and electron microscopic levels and to assay its movement on actin filaments. Our results reveal that ER vesicles, identified by an antibody to the ER-specific resident protein, ECaSt/PDI (Lucero et al., 1994), moved on exogenous actin filaments after isolation and have myosin-V on their surfaces. Experiments were performed to show that vesicle transport on actin filaments was blocked by myosin V specific antibodies. Therefore, we have been able to show that ER vesicles are transported on actin filaments and the movement is driven by an unconventional myosin of the type V class.

MATERIALS AND METHODS

Materials

Squid (*Loligo peali*) were obtained from the Marine Resource Center of the Marine Biological Laboratory (Woods Hole, MA). Monomeric rabbit skeletal muscle actin was prepared according to the method of Pardee and Spudich (1982). Bovine brain calmodulin was purchased from Calbiochem, $DiOC_6$ from Molecular Probes, the primary antibody to human platelet myosin-II from Biochemical Technologies (Stoughton, MA), fluorescently labeled secondary antibodies from Jackson Immunochemicals, and colloidal gold-labeled secondary antibodies from E-Y Laboratories. The antibody to ECaSt/PDI was obtained from Benjamin Kaminer, the antibody to chick brain myosin-V from Mark Mooseker, the polyclonal antibody to the head domain of chicken myosin-V from Roy Larson, the antibody to kinesin heavy chain from Scott Brady and the monoclonal antibody to dynein intermediate chain (M74-2) from Walter Steffen. Rhodamine-phalliodin, nocodazole and papain bound to agarose beads were purchased from Sigma Chemical Company (St Louis, MO). Purified squid myosin-V was used to make a rabbit polyclonal antibody (Cocalico Biologicals, Inc., Reamstown, PA) and a 16 amino acid peptide (QLLQPRKTDADVDSVC) in the globular tail domain (Molyneaux and Langford, 1997) was used to produce a function-blocking antibody to myosin V (αQLLQ). Fab fragments of αQLLQ were prepared according to the method of Mage (1980).

Squid giant axon dissection, extrusion and ghost preparation

Giant axons were dissected and extruded as previously described (Allen et al., 1985; Weiss et al., 1988). Axoplasmic ghosts were prepared by an adaptation of the method of Morris and Lasek (1982). Briefly, dissected and cleaned giant axons were extruded onto parafilm and the axoplasm was immediately transferred into 2 ml of ice-cold TAMD buffer (25 mM Tris-HCl, pH 7.5, 5 mM ATP, 5 mM $MgCl_2$, 2 mM DTT, with 30 μM nocodazole). Axoplasm was incubated on ice for 2 hours and the buffer-extracted axoplasmic ghost was removed with fine dissecting forceps.

Actin-based organelle motility in axoplasm

Organelle motility in intact axoplasm was observed by extruding axoplasm on a coverslip and incubating in TAMDC buffer (TAMD with 25 μg/ml calmodulin) containing 0.4 μM rhodamine-phalloidin (rh-ph) in a humid chamber at room temperature. Within 1 hour, actin-based organelle motility was examined by Allen video-enhanced contrast differential interference contrast (AVEC-DIC) microscopy (Allen et al., 1981, 1985; Weiss et al., 1989) and the presence of actin filaments was confirmed by video intensified fluorescence microscopy (Weiss et al., 1989). Average and instantaneous velocities of moving organelles were calculated by extracting the x and y coordinates of moving organelles from digitized series of video images. The levels of actin-based motile activity (number of vesicles moving/field per minute) was determined by counting the total number of organelles exhibiting directed motion on tracks invisible by AVEC-DIC microscopy. Four areas of the preparation between 20 and 60 μm apart were selected for analysis and the number of moving organelles in each area was tabulated for 15 second intervals. When measuring velocities and motile activity for ER, only vesicles that were obviously part of a larger complex (tethered vesicles with visible tubular elements or vesicles that remain in focus for extended periods without diffusing into the bulk solution) were counted.

Movement of isolated tubulovesicular organelles on exogenous rabbit skeletal muscle actin filaments

Rh-ph rabbit muscle F-actin coated coverslips were prepared as previously described (Kuznetsov et al., 1994). Tubulovesicular organelles (TVOs) from axoplasm were prepared as axoplasmic ghosts and were incubated in TAMDC with rh-ph F-actin coated coverslips for 30 minutes to allow organelles to bind to the actin network. Coverslips were then mounted on slides and motility was observed by AVEC-DIC microscopy.

Immunofluorescence and laser confocal microscopy

TVOs from axoplasmic ghost preparations were fixed for 1 hour at room temperature in 2 ml phosphate buffered saline (PBS) containing 1% formaldehyde and 0.05% glutaraldehyde. Fixed TVOs were then washed 5 times in excess PBS, incubated for 1 hour at room

temperature with diluted primary antibody (anti-squid myosin-V at 1:1,000; anti-sea urchin ECaSt/PDI at 1:100) in PBS containing 2% bovine serum albumin (PBS/BSA), washed 5 times in PBS, incubated 1 hour at room temperature with fluorescently labeled secondary antibody in PBS/BSA, and again washed 5 times with excess PBS. Labeled TVOs were then mounted on slides using tape spacers to preserve the 3-dimensional structure of the TVOs. Fluorescently labeled TVOs were imaged using either a Bio-Rad or a Zeiss laser scanning confocal microscope system. All images were collected using Zeiss Planapo ×100 (N.A. 1.3) oil immersion objective. Images were transferred to an Apple MacIntosh 7100 computer and contrast enhanced using Adobe Photoshop and NIH/Image image processing software.

Electron and immuno-electron microscopy

To examine the fine structure of vesicles in the axoplasmic ghosts, samples in 5 μl of TAMDC were applied to Formvar/carbon-coated copper grids and negatively stained using 1% aqueous uranyl acetate. Grids were examined in a Zeiss 10C electron microscope. Samples processed for immuno-electron microscopy were negatively stained after incubation in colloidal gold-labeled secondary antibodies.

Antibody inhibition of actin-based vesicle motility

The antibody inhibition experiments were conducted as follows. Freshly dissected axons were cut in half and one half was extruded onto a coverslip in 14 μl TAMD buffer containing the control antibody and the other in buffer containing the experimental antibody. A monoclonal antibody to the intermediate chain of dynein (Steffen et al., 1996) and Protein A purified rabbit IgG were used as controls at the same concentration as the experimental antibody. The αQLLQ antibody was used at concentrations of 0.75 and 1.0 mg/ml. Fab fragments of the αQLLQ antibody were used at a concentration of 0.75 mg/ml. The polyclonal antibody to the head domain of chicken myosin V was used at a concentration of 0.9 mg/ml. Movement of vesicles on actin filaments in the experimental and control samples were recorded on videotape and the motile activity determined after 30 minutes. The presence of actin filaments was confirmed by fluorescence microscopy after staining with rh-ph.

SDS-polyacrylamide gel electrophoresis and immunoblotting

Samples of axoplasm and axoplasmic ghost preparations were electrophoresed on 7% and 5-20% gradient SDS polyacrylamide gels according to the method of Laemmli (1970) and were transferred to nitrocellulose membranes using a semi-dry blotting apparatus. The nitrocellulose membranes were immunostained using 1:10,000 diluton of anti-squid myosin-V, 1:1,000 anti-sea urchin ECaSt/PDI, 1:2,500 anti-kinesin and 1:2,000 anti-QLLQ. Immunoblots were developed using ECL chemiluminecent system from Amersham Life Science, Inc.

Myosin-V purification from squid optic lobes

Myosin-V was isolated from squid optic lobes (Cohen et al., 1994) using a protocol similar to that used to isolate myosin-V from chick brain (Cheney et al., 1993a). Briefly, optic lobes from 200 live squid were dissected and homogenized in 500 ml H buffer (40 mM Hepes, pH 7.9, 10 mM EDTA, 5 mM ATP, 2 mM DTT, 0.3 mM PMSF) and centrifuged 13,000 rpm in a Beckman GSA rotor for 60 minutes at 4°C. The actin-myosin-V complex in the supernatant (S1) was precipitated by adding 4 M NaCl to bring the final concentration to 0.6 M NaCl then incubating on ice for 60 minutes. The precipitate was pelleted at 13,500 rpm in a Beckman JA-14 rotor for 60 minutes at 4°C. The pellet (P2) was resuspended in 9 ml W buffer (25 mM imidizole·HCl, pH 7.2, 5 mM K-EGTA, 5 mM K-EDTA, 2 mM DTT) and membranes were solubilized by adding 10% Triton X-100 to bring the final concentration to 1% Triton X-100. The pellet was briefly homogenized at 37°C and was centrifuged at 18,000 rpm in a Beckman JA-14 rotor for 20 minutes at 4°C. To remove residual Triton X-100, the pellet (P3) was resuspended in 10 ml of W buffer and centrifuged at 18,000 rpm in a Beckman JA-14 rotor for 20 minutes at 4°C. To solubilize the myosin-V from the actin, the pellet (P4) was resuspended in 400 μl S buffer (25 mM Tris-HCl, pH 8.0, 600 mM NaCl, 10 mM $MgCl_2$, 2 mM EGTA, 10 mM ATP, 2 mM DTT), and was incubated on ice for 60 minutes. The actin was pelleted at 42,000 rpm in a Sorvall RP120AT rotor (100,000 ***g***) for 30 minutes at 4°C and the supernatant (S5) was saved. Aliquots from all pellet and supernatant fractions were saved for analysis by SDS-gel electrophoresis (Laemmli, 1970). S5 contained approximately equal amounts of actin and myosin-V, along with several minor proteins at both high (>200 kDa) and low (<45 kDa) molecular masses. S5 was subject to preparative SDS-gel electrophoresis and the band corresponding to 196 kDa was excised and frozen.

Peptide microsequencing

The 196 kDa polypeptide was excised from SDS-PAGE gels and subjected to in situ proteolytic digestion with trypsin according to the method of Moritz et al. (1995). The resulting peptides were purified by 2 RP-HPLC steps prior to sequencing on a Model 477A Protein Sequencer (Applied Biosystems, Foster City, CA).

RESULTS

Isolation of ER from axoplasm

Movement of organelles on actin filaments in dissociated axoplasm has been well documented (Kuznetsov et al., 1992, 1994; Langford et al., 1994) but reconstitution of movement of a purified vesicle fraction in the absence of cytosolic factors has been difficult to achieve. Nevertheless, reconstitution of movement of purified vesicles in vitro is the best method for determining the types of myosins bound to organelles and identifying soluble factors required for movement. Therefore we developed a procedure to isolate a vesicle fraction from the axoplasm of the squid giant axon that retained motility in an in vitro motility assay for studies of organelle-associated myosins.

An enriched fraction of axoplasmic vesicles was obtained by incubating axoplasm (approx. 5 μl) in a large volume of axoplasmic buffer (2 ml) at 0°C for 2 hours to remove all soluble proteins, actin filaments, microtubules and freely diffusible organelles including mitochondria (Morris and Lasek, 1984). Using this extraction protocol, a uniform

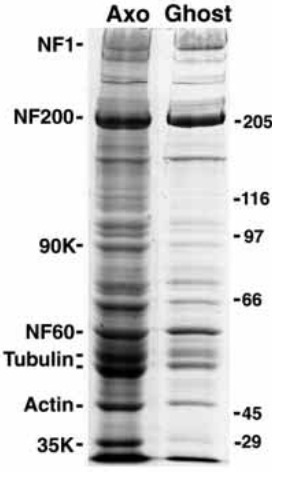

Fig. 1. SDS-polyacrylamide gel of axoplasm and the axoplasmic remnant or ghost. Squid axoplasm was extracted in buffer for 2 hours at 0°C and the protein composition of the ghost compared to whole axoplasm (Axo). Neurofilament proteins (NF1, NF200, NF60) were retained in the ghost but soluble proteins including tubulin and actin were extracted.

population of vesicles was obtained in a remnant called the axoplasmic ghost. We found that this gentle isolation procedure preserved the motility of these organelles on actin filaments (see below) while traditional methods, such as homogenization followed by density gradient centrifugation, destroyed motility.

The protein composition of the ghost was analyzed by SDS-PAGE and compared to whole axoplasm (Fig. 1). Neurofilament proteins were the major components of the ghost as previously shown by Morris and Lasek (1982, 1984). The extraction procedure removed soluble proteins, including tubulin and actin, to very low levels as determined by Coomassie blue-stained gels. Therefore, this procedure effectively extracted soluble proteins leaving behind the neurofilament cytoskeleton and a reticular network of vesicles that were identified as ER (see below). The morphology of the reticular network of vesicles in the ghost was analyzed by light and electron microscopy.

ER vesicles tethered by 20 nm membrane tubules

Transmission electron microscopy (EM) was used to study the ultrastructure of the reticular network of vesicles in axoplasmic ghosts. Samples were placed on carbon-Formvar coated grids and negatively stained with uranyl acetate. Negative staining was found to be the most effective way to visualize the vesicles in the ghost preparations although the final drying step caused the vesicles to collapse. The electron micrographs showed that the ghosts contained a reticular network of membrane tubules and vesicles (Fig. 2). Neurofilaments (NFs) were the only cytoskeletal components remaining in the axoplasmic remnant.

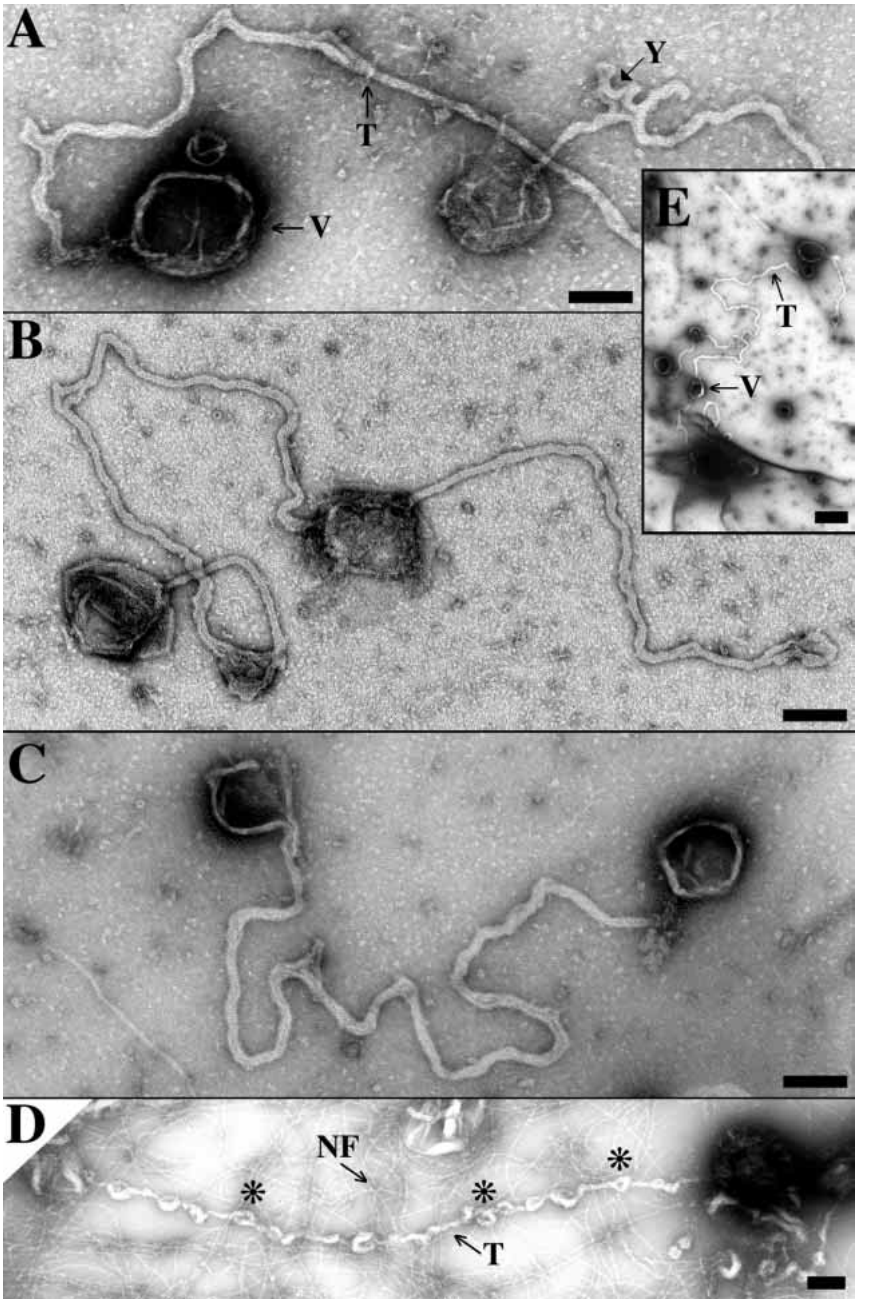

Fig. 2. Negative contrast electron micrographs of ER vesicles from squid axoplasm. (A-C) High magnification and (D-E) low magnification images of tubulovesicular organelles, comprised of vesicles (labeled V) ranging between 100 and 500 nm in diameter attached to tubular membranes (labeled T) 20-25 nm in diameter and several μm in length. Vesicles were usually seen at the ends of the tubular elements, but were occasionally found along the tubular membrane. The tubular membranes often branched to form y-intersections (Y). Also, the tubular membrane coiled into spirals (asterisks in D). These membrane coils may give these tubulovesicular organelles the elastic property that is seen during actin-dependent movement. Neurofilaments (labeled NF) were seen in the background. Bars, 100 nm.

Actin filaments were not present in the axoplasmic ghost and microtubules were rarely seen (Tabb et al., 1996). Actin filaments could be preserved as a component of the ghost if the axoplasm was extracted in the presence of phalloidin (data not shown) illustrating that actin filaments are components of the neuronal cytoskeleton. The actin filaments in such preparations were between 0.5 and 1.0 μm in length and showed no special relationship with organelles or NFs.

The vesicles of the reticular network were connected to each other by long thin membrane tubules. The vesicles ranged between 100 and 500 nm in diameter and were most often located at the ends of tubules although occasionally, a vesicle was found along a tubule (Fig. 2). One of the most striking features of the tubular membranes was their uniform diameter of 20-25 nm. Tubules occasionally branched to form Y intersections and a given tubule could reach several micrometers in length. A frequent configuration was a long tubule that coiled at regular intervals along its length (Fig. 2D). Each coiled region was a 360° turn of the tubule forming a helix or spiral and a series of equally spaced helixes produced a beaded appearance of the tubule. The spiral configuration may have been responsible for the recoil that occurred during cycles of movement (see below).

ER vesicles moved on exogenous actin filaments in vitro

The morphology and motility of the isolated vesicles identified as ER (see below) were examined by AVEC-DIC microscopy. In axoplasmic buffer, the reticular networks appeared as clusters of vesicles that were in either a compact or an extended configuration (Fig. 3). When in the compact configuration, the individual vesicles within a cluster were too closely spaced to be distinguished except at the margins of the cluster (Fig. 3A). When in the extended configuration, vesicular and tubular elements could be easily detected (Fig. 3B-D). The relationship of the two configurations is unclear but they may represent different levels of interaction with the NF cytoskeleton and this interaction may have functional significance. Since the membrane tubules and microtubules are of similar diameter, tubule thickness could not be used to differentiate the two, but the pattern of vibration resulting from Brownian forces could be used. Random thermal motion caused the membrane tubules to vibrate with high frequency undulations while microtubules remained stiff and inflexible. Therefore, contaminating microtubules in these preparations were easy to identify when present. Nocodazole was included in the extraction buffer to promote microtubule disassembly, therefore microtubules were rarely found. The vesicles at the ends of the membrane tubules moved randomly in solution as a result of Brownian forces. Even when the membrane tubules were not visible, it was possible to establish that the vesicles were part of a reticular network because they remained in the field of view for extended periods of time. By contrast, a free independent vesicle undergoing Brownian motion would rapidly leave the focal plane.

A motility assay was developed by adsorbing skeletal muscle actin filaments to a glass coverslip (Kuznetsov et al., 1994) then adding the isolated vesicles. Movement of isolated ER vesicles on the actin-coated coverslips was observed by AVEC-DIC microscopy which is capable of detecting vesicles as small as 50 nm. To visualize the actin filament network, actin filaments were stained with rhodamine-phalloidin and viewed by fluorescence microscopy. Isolated vesicles were placed on the actin-coated coverslips in buffer containing ATP. After incubation at room temperature for 10-15 minutes, movement was detected and recorded on videotape for subsequent motion analysis. ATP was required for movement but the addition of soluble factors was not required.

The isolated ER vesicles moved on actin filaments along a complex path that zigzagged as the vesicle moved from filament to filament (Fig. 4). Typically the vesicle attached to an actin filament and moved at an average velocity of 0.7±0.3 μm/second (Table 1), a rate that was similar to that of vesicles moving on actin filaments in extruded axoplasm (Kuznetsov et al., 1994). As the vesicle moved along the actin filament, the tubular membrane became extended until the movement stopped. Often, the vesicle detached from the actin filament and snapped backward due to the elastic recoil of the stretched membrane tubule. In many cases, the vesicle reattached to either the same or another actin filament and began the cycle of movement, detachment, rapid recoil and reattachment several times. In cases where the vesicle snapped back, the rapid reversal of movement of vesicles was due to the elastic property of the tubules likely resulting from its helical form. The coiled tubules stretched like a spring during movement on the actin filament and recoiled when the vesicle detached.

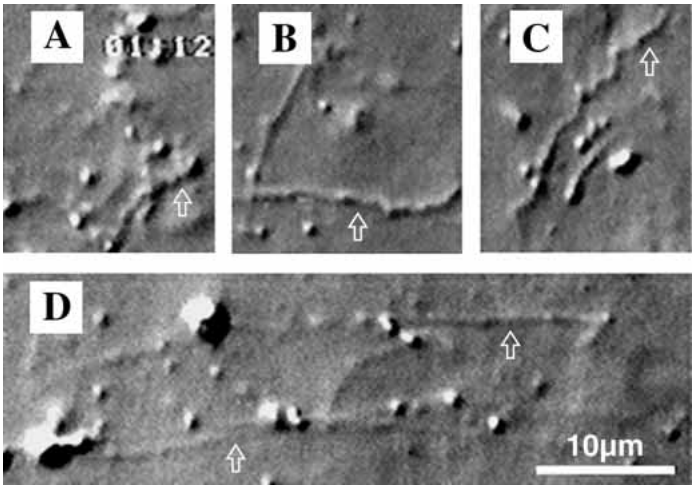

Fig. 3. AVEC-DIC micrographs of ER vesicles from axoplasmic ghosts. (A) A compact ER network consisting of multiple vesicles and contracted membrane tubules (arrow). (B) Extended ER network with numerous small vesicles and long membrane tubules (arrow). Note the uniform diameter of the membrane tubules. Vibrations of the membrane tubules due to thermal motion provided a means to distinguish tubular membranes from stiffer microtubules. (C) A group of ER vesicles with wavy tubular membranes (arrow) and vesicles of small and intermediate sizes. (D) A large extended network of ER. The tubular membranes (arrows) extended along the glass coverslip for more than 40 μm.

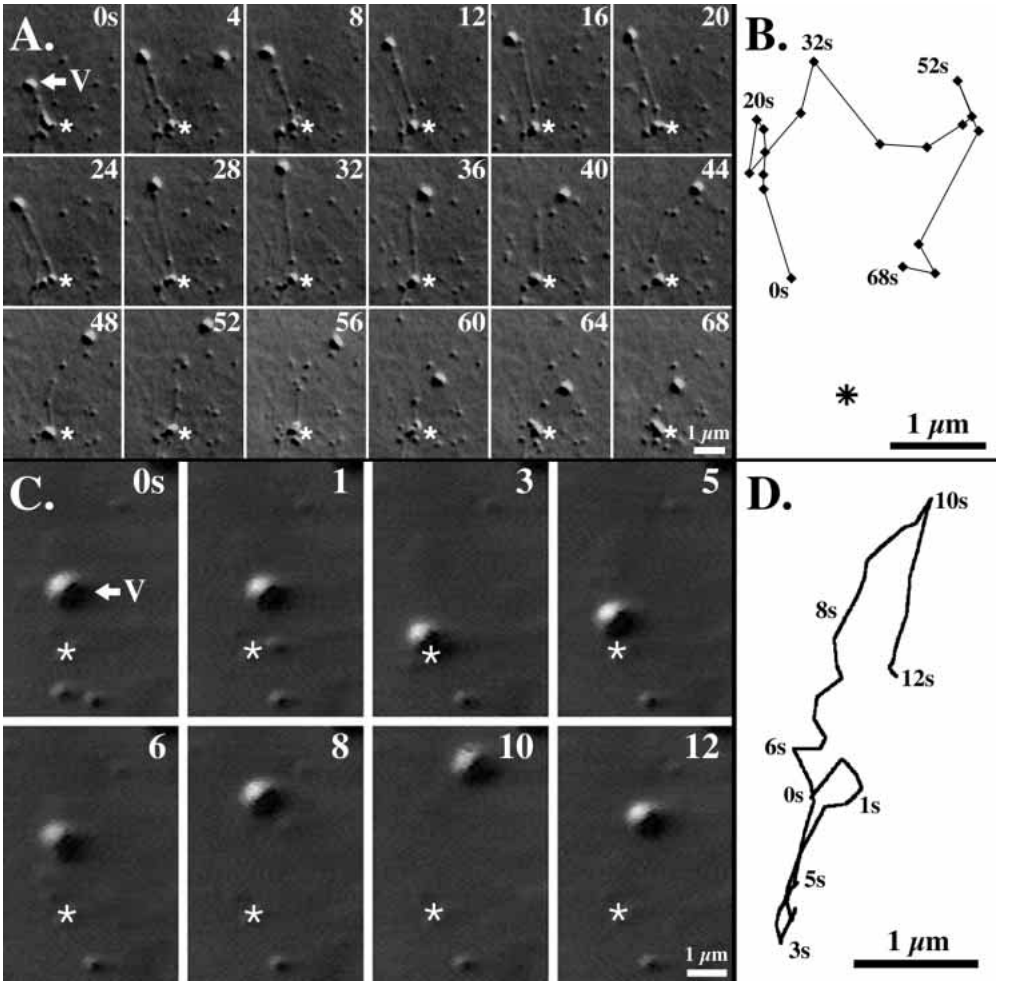

Fig. 4. Actin-dependent movement of ER in intact axoplasm and isolated ER on exogenous actin filaments. (A) Video microscopy images of an ER vesicle in extruded axoplasm moving on rhodamine phalloidin-labeled actin filaments. Since actin filaments are smaller than the detection level of AVEC-DIC microscopy, the organelles appeared to move on invisible tracks. The presence of actin was verified by fluorescence microscopy (data not shown). Asterisk denotes where the ER attached to the glass coverslip. The large vesicle moved from the site of attachment during the first 20 seconds, retracted briefly, extended forward until 32 seconds, retracted again, extended until 52 seconds and then retracted again. Note that the tubular membrane was clearly visible when the vesicle moved forward from the site of attachment. (B) Diagram of the path of the vesicle shown in A. (C) Video microscopy images of an isolated ER vesicle moving along rhodamine-phalloidin-labeled rabbit skeletal muscle actin filaments. Asterisk denotes where the ER was attached to the glass coverslip. (D) Diagram of the path of the vesicle shown in C; the vesicle exhibited cycles of forward movement followed by retraction to the site of attachment (the tubular membrane is out of the plane of focus, and therefore cannot be seen).

These results demonstrated that isolated vesicles retained the ability to move on actin filaments in the absence of soluble cytosolic factors. We conclude, therefore, that the myosin motors required for movement are tightly bound to these organelles and should be localized to their surfaces.

Antibody to ERcalcistorin/protein disulfide isomerase (ECaSt/PDI) used as ER-marker

The morphology of the reticular network of vesicles as revealed by both EM and light microscopy resembled smooth endoplasmic reticulum (ER). To demonstrate that the tubular and vesicular elements were part of a continuous network and to ensure that the tubules seen by DIC microscopy were membrane and not microtubules, we stained the samples with the fluorescent dye, $DiOC_6$. This dye has been used extensively to study ER in cultured cells, eggs and oocytes (Terasaki et al., 1984; Terasaki and Jaffe 1993). In axoplasmic ghosts treated with 2.5 μg/ml $DiOC_6$, both the vesicular and tubular domains of the reticular networks stained brightly fluorescent. Confocal micrographs of these preparations (Fig. 5A) showed the complex arrangement of vesicular and tubular elements present within the axoplasmic ghosts. By comparing fluorescent micrographs with DIC images of the same vesicles (Fig. 5B,C), it was possible to demonstrate that both the vesicular and tubular domains were labeled with $DiOC_6$. Therefore both domains were composed of membranes.

While light and electron micrographs of the vesicles suggested that they resembled endoplasmic reticulum, more rigorous proof was needed. Therefore, to demonstrate unequivocally that these vesicles are endoplasmic reticulum, we

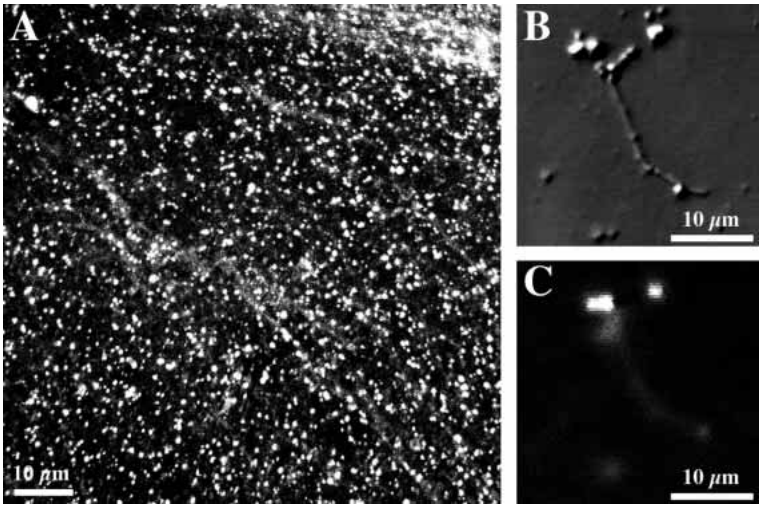

Fig. 5. Fluorescence micrographs of ER vesicles stained with $DiOC_6$. (A) Axoplasmic ghosts were incubated in 2.5 μg/ml $DiOC_6$ and imaged by confocal microscopy. Vesicles of various sizes are seen and the vesicles appear to align in linear arrays. (B) AVEC-DIC microscopy image of a small fragment of ER, containing several vesicles and tubules. (C) A fluorescence micrograph of the same ER fragment in B. Both the vesicles and the tubules stain with $DiOC_6$, indicating that they are both comprised of membrane.

used an antibody to an ER-specific protein purified from sea urchin eggs, called ERcalcistorin/protein disulfide isomerase (ECaSt/PDI) (Lucero et al., 1994, 1998). The ECaSt/PDI antibody cross-reacted with a single, 58 kDa protein in extruded squid axoplasm and the axoplasmic ghost on immunoblots (Fig. 6A). This antibody was used as a probe to detect ECaSt/PDI in the reticular network of vesicles by immunofluorescence microscopy. Confocal micrographs of formaldehyde-fixed and detergent-permeabilized vesicles stained with the ECaSt/PDI antibody showed that the vesicular domains were fluorescent, indicating the presence of ECaSt/PDI (Fig. 6B). Direct comparison of fluorescent and DIC images of the same vesicles showed that vesicles detected by DIC, were also labeled by the ECaSt/PDI antibody (Fig. 6C,D). Fluorescence was not detected in control samples that were treated either with pre-immune serum or a buffer wash in place of the primary antibody. Since ECaSt/PDI is a protein that is found in the endoplasmic reticulum (Lucero et al., 1994), these results demonstrate that the reticular network of vesicles isolated from the squid giant axon are elements of the ER (the Golgi may contain ECaSt/PDI but it is not located in axons).

Table 1. Average velocity and motile activity of organelles on actin filaments

Organelles	Average velocity (μm/second)	Motile activity (moving vesicles/ field per minute)
Small vesicular organelles*,‡ (d<400 nm)	0.9±0.3 (*n*=51)	60-130§
Medium vesicular organelles*,‡ (d=400-800 nm)	0.7±0.3 (*n*=35)	n.d.
Tubulovesicular organelles‡	0.7±0.3 (*n*=98)	37±11 (*n*=8)
Isolated ER vesicles	1.0±0.4 (*n*=33)	23±8 (*n*=6)

*Data from Kuznetsov et al., 1994.
‡Measured in extruded axoplasm.
§Range of motile activities for organelles of all sizes; from Kuznetsov et al., 1994.
n.d., not determined.

Myosin V is located on ER vesicles

The myosin motor located on the surfaces of the ER vesicles was identified as follows. Blots of axoplasm were probed with antibodies generated against several known myosins. We found that an antibody to chick brain myosin V (Espindola et al., 1992), a type of myosin that is known to be abundant in brain, showed cross-reactivity with a 196 kDa protein in axoplasm (Fig. 7A, lane 1).

We purified the protein recognized by this antibody from squid brain by a method similar to that of Cheney et al. (1993a). The purified 196 kDa protein (p196) exhibited calcium-stimulated, actin-activated ATPase activity similar to that reported for chicken myosin V, providing evidence that it was a myosin (Cohen et al., 1994; manuscript in preparation). Trypic fragments of p196 were micro-sequenced and the amino acid sequences of the peptide fragments were compared to the amino acid sequences of myosin V from mouse, chicken, rat and yeast. The amino acid sequences of peptides that aligned in the head domain showed approximately 95% identity/similarity to the other members of the myosin V class (Table 2). The sequences that aligned with myosin-V tail sequences showed less identity/similarity (50%) as expected because the tail domains have been shown to be more variable among species (Cheney et al., 1993b). These sequences provided definitive evidence that squid brain p196 is a member of the myosin V class of proteins. RT-PCR was used to generate 2 fragments of the squid myosin-V gene and the sequences of these fragments were homologous to chicken myosin-V (unpublished).

A rabbit polycolonal antibody was generated to purified squid myosin V (Fig. 7A, lane 5) and the antibody showed reactivity with a single band on blots of axoplasm and axoplasmic ghosts. The specificity of this antibody for myosin V was demonstrated by running samples of axoplasm on a gradient gel that allowed the clear separation of the 210 kDa myosin-II band and the 196 kDa myosin-V band. The 210 kDa band was confirmed to be myosin-II by its reaction with an antibody to human platelet myosin-II (Fig. 7A, lane 2). The squid myosin-V antibody recognized only the 196 kDa band on blots of axoplasm and axoplasmic ghosts (Fig. 7A, lanes 3 and 4). The squid myosin-V antibody was used to detect the

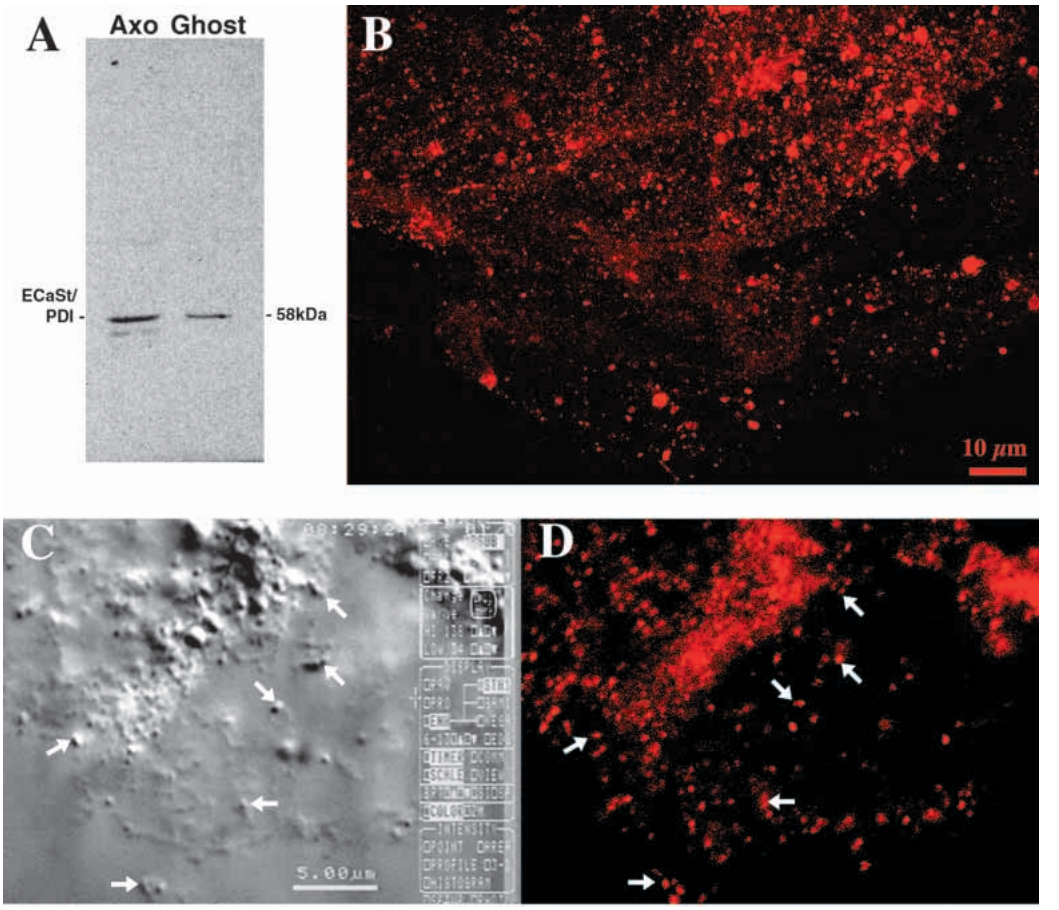

Fig. 6. ER stained with an antibody to ER calcistorin/protein disulfide isomerase (ECaSt/PDI), an endoplasmic reticulum specific protein. (A) The antibody to sea urchin embryo ECaSt/PDI showed cross-reactivity with a single protein of 58 kDa in both axoplasm and axoplasmic ghosts on immuno-blots. (B) Confocal micrograph of fixed and permeabilized axoplasmic ghosts treated with anti-ECaSt/PDI primary antibody and rhodamine-labeled secondary antibody. The ECaSt/PDI antibody stained vesicles of various sizes, but tubular membranes were not stained. Control samples that were treated with pre-immune primary antibody or without primary antibody did not show labeling. (C and D) DIC and conventional fluorescence micrographs of an axoplamic ghost treated with anti-EcaSt/PDI. The same field is shown to illustrate that most vesicles visible by DIC were stained with the ER-specific marker antibody. The arrows indicate the location of the corresponding points in the two images. Bar, 5 μm.

presence of myosin V on ER in the ghost preparations. Axoplasmic ghosts were fixed with formaldehyde and incubated with myosin-V antibody followed by rhodamine-labeled secondary antibody. In images obtained by confocal microscopy, antibody-labeled ER vesicles appeared as bright punctate structures against a dark background (Fig. 7B). The fluorescently labeled vesicles were of various sizes and were often aligned in rows. All vesicles visible by AVEC-DIC microscopy were visible as fluorescent objects indicating that myosin V motors were bound to these ER vesicles.

In addition to fluorescence microscopy, immunogold electron microscopy was used to demonstrate the localization of myosin V on ER vesicles and to demonstrate the co-localization of myosin V and the microtubule motor kinesin. Axoplasmic ghosts were fixed with formaldehyde then reacted with the polyclonal antibody to squid myosin V (Tabb et al., 1996) and a monoclonal antibody to squid kinesin heavy chain (Brady et al., 1990; Leopold et al., 1992). The labeled ghosts were incubated with 10 nm gold-labeled anti-rabbit secondary antibody for the myosin antibody and 20 nm gold-labeled anti-mouse secondary antibody for the kinesin antibody. The gold-labeled ghosts were transferred to a carbon-Formvar coated grid and stained with uranyl acetate. Control ghosts were prepared by substituting a buffer wash or preimmune serum for the primary antibodies. By the negative staining EM technique, membrane organelles could be positively identified as distinct from the surrounding neurofilaments (Tabb et al., 1996).

The distribution of the 10 nm and 20 nm collodial gold beads in micrographs was analyzed and 85-90% of the gold was found to be localized to structures that could be positively identified as ER vesicles (Fig. 8A-D). Both 10 nm and 20 nm collodial gold beads were found on the same vesicles, demonstrating the colocalization of myosin and kinesin motors (Fig. 8A-D). Most of the gold beads localized to the ER vesicles and not the membrane tubules. We cannot rule out the possibility that motors may be distributed along the tubular membrane elements because the number of motors on these elements may be below the limit of detection by this technique. The number of 10 nm gold beads (myosin-V) on organelles ranged from 6 (for a small vesicle; inset Fig. 8B) to 120 (for a

Table 2. Comparison of the amino acid sequences of head and tail peptides of squid p196 with sequences of other myosin-Vs

Head sequences															
Squid p196		L	A	S	N	P	I	M	E	S	F	G	N	A	K	
Mouse Myo-V	197	L	A	S	N	P	I	M	E	S	I	G	N	A	K	210
Chicken Myo-V	197	L	A	S	N	P	I	M	E	S	I	G	N	A	K	210
Rat Myr 6	197	L	A	S	S	P	I	M	E	A	I	G	N	A	K	210
Yeast Myo2	206	L	A	T	N	P	I	M	E	A	F	G	N	A	K	219
Yeast Myo4	205	L	A	T	N	P	I	M	E	A	F	G	N	A	K	218
Tail sequences															
Squid p196		A	V	D	P	E	V	I	T	L	I	V	K			
Mouse Myo-V	1,677	G	M	D	P	E	L	I	K	Q	V	V	K			1,688
Chicken Myo-V	1,653	G	M	D	P	E	L	I	K	Q	V	V	K			1,664
Rat Myr 6	1,670	G	L	D	P	E	I	I	L	Q	V	F	K			1,681
Yeast Myo2	1,373	H	I	E	N	E	V	F	H	A	V	V	T			1,384
Yeast Myo4	1,291	Q	V	V	D	S	M	H	T	K	I	F	N			1,302

The sequences of two squid p196 peptides were compared to myosin-V amino acid sequences in database (myo 2 and myo 4 are the yeast members of the myosin-V family). Identical amino acids are boxed in white, highly similar amino acids are darkly shaded and similar amino acids are lightly shaded. Head domain peptides from squid show high identity/similarity (85-90%) to mouse, chicken, rat, and yeast myosin-V, while squid tail doman peptides show 50% identity/similarity to mouse and chicken and 42% to rat myosin-V sequences. The squid tail peptide shows little similarity to yeast myosin-V sequences.

large vesicle). Fewer 20 nm gold beads (kinesin) were seen on vesicles in these micrographs (Fig. 8A-D). The number of gold beads on vesicles processed with a single primary antibody (Fig. 8E) was similar to the number of gold beads found on vesicles processed with the two primary antibodies (Fig. 8A-D). In control samples (Fig. 8F), the number of 10 nm gold beads (myosin-V) on vesicles was not above background (usually <8).

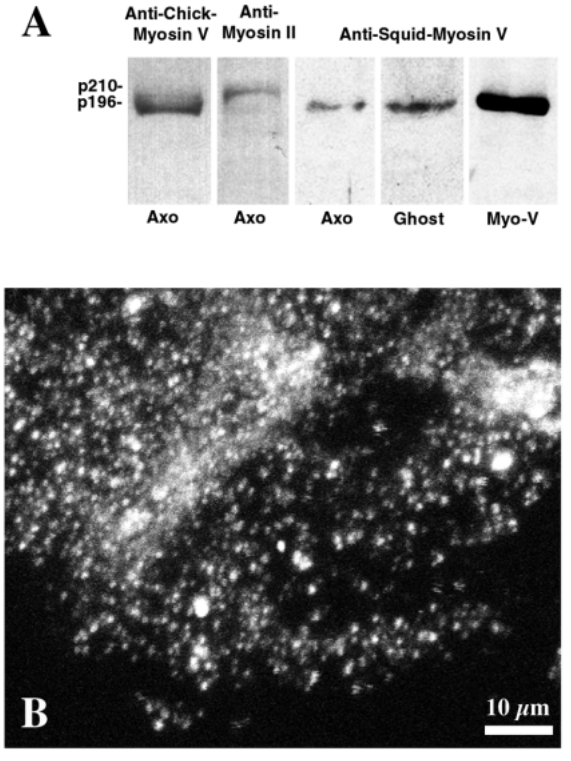

Fig. 7. Immunoblots and micrograph of ER probed with myosin-V antibodies. (A) Antibody to chick brain myosin-V cross-reacted with a single protein of 196 kDa in extruded axoplasm (lane 1, Axo). An antibody to human platelet myosin-II was used to identify the 210 kDa myosin II in axoplasm (lane 2, Axo). The myosin V-specific antibodies did not cross-react with myosin II. The rabbit polyclonal antibody generated against squid optic lobe myosin-V reacted only with the 196 kDa protein in axoplasm (lane 3, Axo) and axoplasmic ghost (lane 4, ghost). The anti-squid myosin-V gave a strong reaction to purified squid brain myosin-V (lane 5, Myo-V). (B) Confocal micrograph of fixed axoplasmic ghosts treated with anti-squid myosin-V primary antibody and rhodamine-labeled secondary antibody. The myosin-V antibody stained vesicles of various sizes. Control samples that were treated with pre-immune primary antibody or without primary antibody did not show labeling.

These data demonstrate that the microtubule motor, kinesin, and the actin filament motor, myosin V, are located on the same ER vesicles. We conclude, therefore, that the co-localization of myosin V and kinesin on the same vesicle provides the means by which a vesicle is able to switch between actin filaments and microtubules during movement.

Inhibition of vesicle transport with a myosin V specific antibody

Antibody inhibition experiments were performed to demonstrate conclusively that myosin V functions as a vesicle motor in the squid giant axon. Two function-blocking antibodies were used in this study. We generated a polyclonal antibody (αQLLQ) to a 16 amino acid peptide in the tail domain of squid brain myosin V (Molyneaux and Langford, 1997) and we obtained a polyclonal antibody (αMyo-V head) made against the motor domain of chicken myosin V (Espreafico et al., 1992). The latter antibody has been shown to inhibit the ATPase activity of myosin V (Wolenski et al., 1995). The amino acid sequence used for αQLLQ production (QLLQPRKTDADVDSVC) was obtained by sequencing a

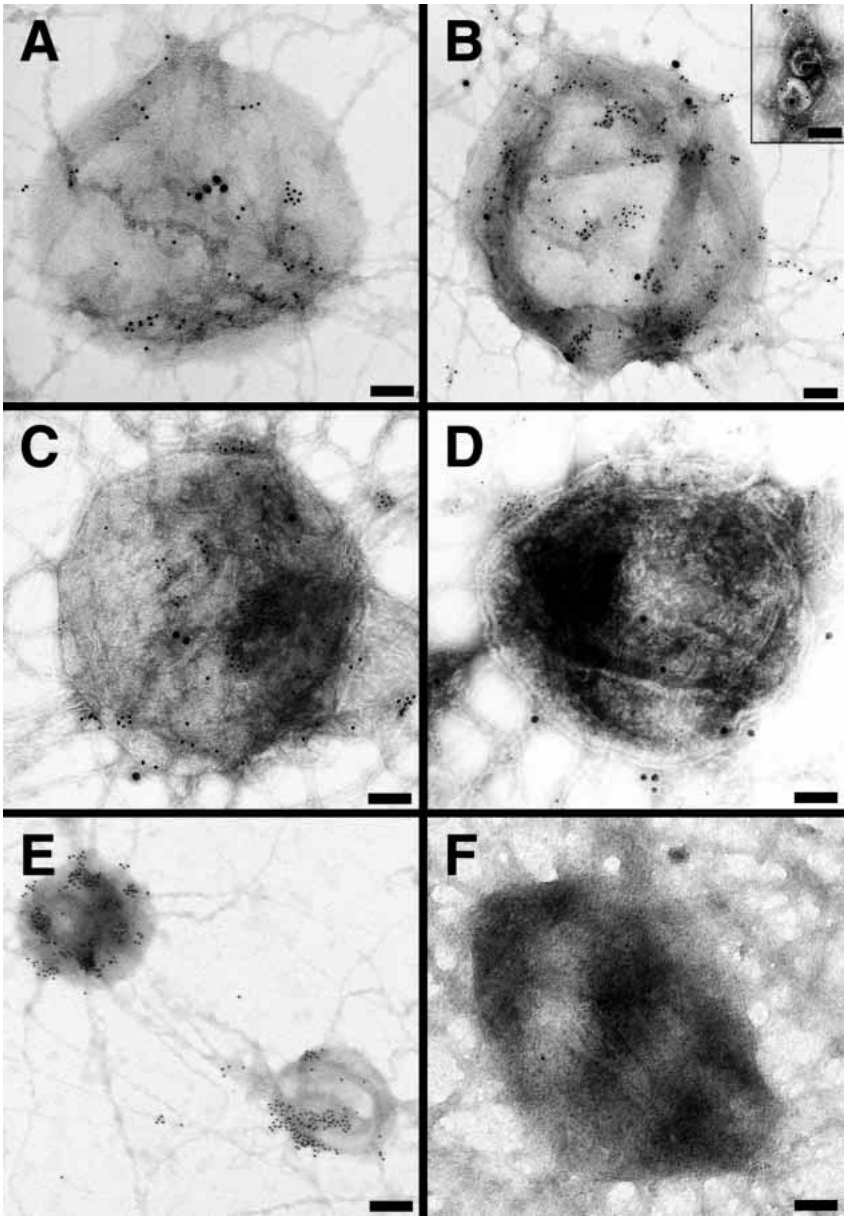

Fig. 8. Electron micrographs demonstrating co-localization of myosin V (small gold beads) and kinesin (large gold beads) on ER vesicles. (A-D) Axoplasmic ghosts were reacted with primary antibodies to squid myosin V and squid kinesin heavy chain then with 10-nm gold-labeled secondary antibody for the myosin antibody and 20-nm gold-labeled secondary antibody for the kinesin antibody. The gold-labeled ghosts were transferred to a carbon-Formvar coated grid and stained with uranyl acetate. Small and large gold beads are found on the same vesicle indicating that both myosin V and kinesin are bound to these veiscles (inset in panel B shows small vesicles). (E) ER was stained for myosin only. (F) The primary antibodies were replaced with pre-immune sera to demonstrate the specificity of the labeling reaction. The co-localization of myosin V and kinesin on the same vesicle provides the means by which a vesicle is able to switch between actin filaments and microtubules during movement. Bars, 100 nm.

cDNA fragment of 650 bp near the 3′-end of the squid brain myosin V gene.

On immunoblots, αQLLQ reacted with a single 196 kDa protein band in fractions of squid brain enriched for myosin V (Fig. 9A, lane 1) and the equivalent band in axoplasm (Fig. 9A, lane 2), demonstrating its specificity for squid myosin V. The αMyo-V head antibody recognized the same protein band in fractions of squid brain enriched for myosin V (Fig. 9A, lane 3). These affinity-purified antibodies were tested for their ability to inhibit actin-based vesicle movement in extruded axoplasm. In all experiments, the axon was divided in half and one half of the axoplasm was treated with a control antibody and the other half with αQLLQ or αMyo-V head. The actin filaments on which the vesicles moved were visualized with fluorescence microscopy. The use of two halves of the same axon for the control and the experimental treatments controlled for the variability in motile activity among axons. The presence of vesicle transport on microtubules in the antibody treated preparations provided a means to ensure that the inhibition was specific to actin-based movement and not the result of a systemic disruption. The inhibition by each antibody was determined for 3 axons and reported as the average motile activity.

Motile activity on actin filaments was inhibited by 84±25% compared to the control when αQLLQ was added at a concentration of 0.75 mg/ml (Fig. 9B). At a concentration of 1.0 mg/ml, the inhibition was 98±4%. The preparations were monitored for 45 minutes although percent inhibition was determined after 30 minutes of treatment. To demonstrate that the inhibition was not a result of immunoprecipitation or cross-linking by the antibody, trials were conducted using Fab fragments of αQLLQ. Inhibition was observed to be 95±6% in these trials, the same as for the intact antibody (Fig. 9B). Antibody inhibition experiments performed with the αMyo-V head antibody gave similar results. When added to axoplasm

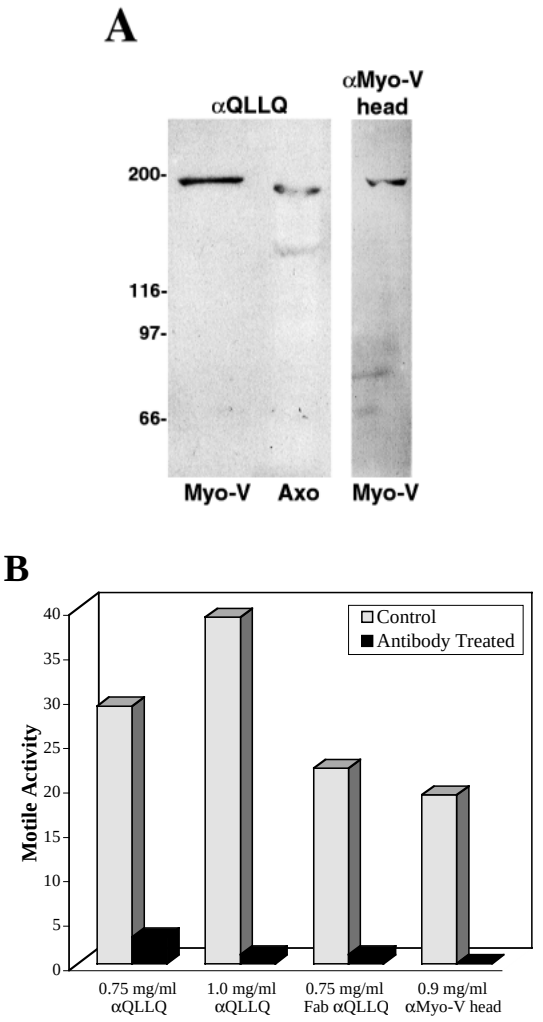

Fig. 9. Antibodies specific to myosin V inhibited vesicle transport on actin filaments. (A) Immunoblots of purified squid brain myosin V (Myo-V) and of extruded axoplasm (Axo) probed with an antibody (aQLLQ) made to a peptide located in the globular tail domain of squid myosin V and an antibody (aMyo-V head) made to the globular head fragment of chicken brain myosin V. Both antibodies recognized myosin V in these samples. The molecular mass markers are indicated to the left of the blots. (B) Motile activity of extruded axoplasm treated with myosin V specific antibodies. Each pair of bars (gray for control antibody and black for myosin V antibody) represents the average motile activity in 3 separate trials. Two concentrations of aQLLQ (0.75 and 1.0 mg/ml), Fab fragments of aQLLQ at 0.75 mg/ml and aMyo-V head at 0.9 mg/ml were used. Vesicle transport on actin filaments (measured after 30 minutes of treatment) was inhibited by greater than 90% in all cases.

at a concentration of 0.9 mg/ml, vesicle movement on actin filaments was inhibited by 98±6% compared to controls (Fig. 9B). These antibody inhibition experiments provide direct evidence that myosin V is the motor responsible for the movement of vesicles on actin filaments in axoplasm.

DISCUSSION

In this study we have shown that ER vesicles isolated from axoplasm of the squid giant axon move on actin filaments. The actin-dependent motor on ER vesicles was identified as myosin V based on comparisons of the sequences of peptides from squid myosin-V and the other members of the myosin V class. Furthermore, myosin V was tightly bound to the membranes of the ER vesicles and was not removed during isolation. Myosin V was shown to co-localize on vesicles with the microtubule-dependent motor kinesin. In addition, antibody inhibition experiments showed that myosin-V specific antibodies blocked movement of vesicles on actin filaments. The antibody inhibition experiments provide direct evidence that myosin V is the motor responsible for the movement of vesicles on actin filaments in axoplasm. Therefore, these data establish the role of myosin-V in fast axonal transport and provide support for the dual filament model of transport.

It is important to note that myosin-V retained its function as an ER motor after extraction of soluble proteins from the axoplasm. The extraction protocol resulted in the dilution of soluble factors by at least 400-fold after the 2-hour incubation period. This extraction procedure was sufficient to reduce soluble proteins to levels undetectable on Coomassie blue stained gels. Neurofilaments were not extracted from the ghosts because these polymers were resistant to depolymerization by cold and dilution. The small amount of tubulin detected in the ghost was present in the form of short segments of microtubules. Actin filaments were not visible in the ghost except when stabilized by phalloidin prior to extraction.

Our previous attempts to purify axoplasmic organelles that retained the ability to move on actin filaments were unsuccessful. These experiments involved homogenization of the axoplasm followed by fractionation of vesicles on sucrose density gradients. Apparently, mechanical disruption of the axoplasm destroyed motile activity. We thought this difficulty was due to the fact that the myosin motors were bound loosely to the membrane and were removed from organelles during homogenization. In this study, we have shown that the myosin motors are tightly bound to ER vesicles. In addition we have shown that soluble factors are not required for movement. Therefore, it remains unclear why homogenization destroyed motility. The most likely explanation is that the motor activity is sensitive to the mechanical fragmentation of organelles in axoplasm. The nature of this sensitivity remains unknown but could be due to the inactivation of motors by a factor that is activated during homogenization. The inability to reconstitute actin-dependent movement of vesicles isolated from homogenates of chicken brain was recently reported (Evans et al., 1998). These authors showed that myosin V was located on some vesicles in the microsome fraction but movement on actin filaments did not occur. Vesicles extracted with detergent and adsorbed to glass coverslips produced actin filament sliding. The basis of the inactivation of myosin V on vesicles in these homogenates and the mechanism of detergent reactivation was not determined.

Myosin V is regulated by calmodulin (Espindola et al., 1992; Cheney et al., 1993a), therefore changes in calcium levels during disruption of cells may alter the light chain composition of the motors or trigger a signaling cascade that results in the inactivation of the motors. With the successful purification of ER vesicles in axoplasmic ghosts, we will be able to investigate the mechanism of motor regulation. In addition, the

discrepancy between the effects of Ca^{2+} on myosin V's ATPase activity (Nascimento et al., 1996; Larson, 1996) and movement of artificial beads (Wolenski et al., 1995) may be addressed.

The antibody inhibition experiments establish that myosin V is not only located on vesicles but its activity is required for vesicle movement. The two antibodies used in this study reacted with different parts of the motor but both effectively blocked the function of myosin V. The αQLLQ antibody was produced to a peptide located in a domain of the protein called the DIL motif, the sequence of which has high similarity among chicken, mouse, *Drosophila* and yeast class V myosin. This motif has been suggested to be the membrane-binding site on the globular tail (Ponting, 1995) and therefore, an antibody that binds at this site is predicted to disrupt the function of the motor. The other antibody was made against the motor domain of chicken myosin V (Espreafico et al., 1992) and has been shown to inhibit the ATPase activity of this myosin (Wolenski et al., 1995). Therefore, myosin V-specific antibodies, one directed against the motor domain and the other against the putative cargo binding domain inhibited movement of vesicles on actin filaments in axoplasm. The ability to block the function of myosin V and inhibit vesicle transport firmly establishes this class of myosin as a vesicle motor.

ERcalcistorin/protein disulfide isomerase (ECaSt/PDI), an ER marker

The vesicles in the axoplasmic remnant were identified as ER by reaction with an antibody to ECaSt/PDI, an ER-resident protein. ECaSt/PDI is a molecular chaperone that assists in the formation of proper disulfide bridges of newly synthesized proteins. It is a KDEL-bearing protein and it works coordinately with BiP, an ATPase capable of interacting with misfolded or unassembled proteins, to assist protein folding within the ER. In view of their function in chaperoning nascent proteins, BiP and PDI were originally thought to be restricted to the rough ER. However, recent results have firmly established that these two proteins are uniformly distributed within the lumen of the entire ER. Therefore ER-resident proteins, BiP and PDI are the best general markers of the ER (Sitia and Meldolesi, 1992).

Myosin V biochemical characterization

Myosin V is one of the best-characterized unconventional myosins (for recent reviews see Mooseker and Cheney, 1995; Larson 1996; Titus, 1997; Langford and Molyneaux, 1998; Mermall et al., 1998). It is a double headed myosin containing two identical heavy chains, each of which has a long neck region that exhibits 6 IQ motifs thought to be binding sites for calmodulin and other light chains. An 8 kDa polypeptide that is homologous to one of the light chains of cytoplasmic dynein (Benashski et al., 1997) has been shown to bind to the tail domain of myosin-V (Espindola et al., 1996). Though not proven, myosin V has been suggested to have properties like kinesin, a motor that has the ability to move for a hundred ATPase cycles along a microtubule without dissociating (Gilbert et al., 1995; Hackney, 1995; Vale et al., 1996). This processivity accounts for the fact that single or relatively few motors are able to transport organelles efficiently (Vale, 1996; Ostap and Pollard, 1996; Howard, 1997). Purified myosin V has high affinity for actin in the presence of ATP (Cheney et al., 1993a; Nascimento et al., 1996) and the ability to generate movement of beads on actin filaments at a rate of 0.5 μm/second (Wolenski et al., 1993, 1995). The rates measured in vitro are similar to the rates of movement of vesicles in axoplasm (Kuznetsov et al., 1992) and in the reconstituted assay reported here (Table 1). This rate of movement is 50-fold faster than that of myosin I whose velocity has been determined to be 0.025 μm/second (Wolenski et al., 1995).

Myosin V as an organelle motor

Although a significant amount of indirect evidence supports myosin V's role as an organelle motor, the inhibition of vesicle transport with an antibody to myosin V as reported here is the first direct demonstration that myosin V is an organelle motor. Similar results were obtained with vesicles isolated from homogenates of chicken brain although in this case, reconstitution of filament sliding required detergent extraction (Evans et al., 1998). Several previous studies implicated myosin-V as an organelle motor. In mature neurons, myosin-V was shown to be associated with punctate structures that appeared to be vesicles (Espreafico et al., 1992) and in cultured neurons from mouse, myosin-V was shown to be associated with vesicles in the growth cones (Evans et al., 1997). In addition, myosin-V was shown to be present in preparations of synaptic vesicles isolated from rat cerebrocortical synaptosomes and inhibition of myosin ATPase activity with 2,3-butanedione monoxime (BDM) blocked neurotransmitter release (Prekeris and Terrian, 1997).

In addition, myosin V has been shown to have a role in organelle movement in vivo based on studies of melanocytes. The dilute mutation (light coat color) in mice has been shown to be due to a mutation of myosin-V leading to a defect in the transport of melanosomes into the dendritic processes of the melanocytes (Mercer et al., 1991). Antibodies to myosin-V have been used to demonstrate by immunofluorescence microscopy that myosin-V is found on the melanosomes of these cells (Provance et al., 1996; Nascimento et al., 1997). Cultured melanocytes that express the dilute form of myosin V show defects in the dispersion of pigment granules (Wu et al. 1997).

Several studies have shown that yeast cells expressing the mutant form of myo2p, a myosin V isotype, exhibited defects in the movement of secretory vesicles into the newly forming bud (Johnston at al., 1991; Govindan et al., 1995). Myo2p has also been implicated in the transport of the yeast vacuole and the proteins Chs3p (a chitin synthase) and SEC4 (a small GTPase), components that distributed improperly in Myo2 mutants (Hill et al., 1996; Santos and Snyder, 1997; Walch-Solimena et al., 1997).

More recently, a study of dilute mice and rats has shown that there is a defect in the distribution of ER in dendritic spines of Purkinje cells (Takagishi et al., 1996; Dekker-Ohno et al., 1996). These studies looked at the distribution of ER in the Purkinje cells of mutant and normal animals by immunochemical methods using an antibody to IP3 receptors as ER marker. The results provided genetic evidence that myosin-V is required for ER localization in dendritic spines and support our direct observations of movement of ER by myosin V.

Recent studies have identified mutations in myosin-V as the basis for the condition known as Human Griscelli disease (Pastural et al., 1997). Human subjects with this disease exhibit

ataxia, lighter pigmentation, opisthotonus and complications including immunodeficiency (Hurvitz et al., 1993). All of these data provide strong support for a role of myosin-V in vesicle transport.

Dual filament model

In this study we have shown that both microtubule-dependent and actin-dependent motors are found on the same ER vesicles. In addition we have provided direct evidence that myosin-V transports ER vesicles on actin filaments in nerve cells. These studies in conjunction with the recent reports that myosin V is localized to synaptic vesicles and to melanosomes as well as the reported defects in the localization of ER to dendritic spines in animals with myosin V mutations, strongly support myosin V's role as an organelle motor in cells. Although one cannot rule out other functions for this motor such as filopodial extension (Wang et al., 1996), organelle transport appears to be one of its primary function. A loss of its function could lead specifically to a loss of proper Ca^{2+} signaling in both the dendrites and axons as well as reduced exocytosis at the presynaptic terminals. The effects on signaling and neurotransmitter release may account for the neurological defects observed in mutant animals and could account for the symptoms associated with Griscelli disease in humans. In summary, these data support a model in which organelles utilize both actin filaments and microtubules for movement from one functional site in the cell to another.

We sincerely thank Ana DePina, Khary Harmon and Lisa Lee for assistance with the experiments. We thank Mark Mooseker for the chick myosin-V antibody, Scott Brady for the kinesin antibody, Benjamin Kaminer for the ECaSt/PDI antibody and Roy Larson for the head domain of chicken myosin V antibody. We especially thank Howard Jaffe and Harold Gainer for sequencing the squid myosin V tryptic peptides. Supported by NSF grant MCB9506279 and MBL Fellowship to J.S.T.

REFERENCES

Allen, R. D., Allen, N. S. and Travis, J. L. (1981). Video-enhanced contrast differential interference contrast (AVEC-DIC) microscopy: A new method capable of analyzing microtubule-related motility in the reticulopodial network of Allogromia laticollaris. *Cell Motil. Cytoskel.* **1**, 291-302.

Allen, R. D., Weiss, D. G., Hayden, J. H., Brown, D. T., Fujiwake, H. and Simpson, M. (1985). Gliding movements of and bidirectional transport along single native microtubules from squid axoplasm: Evidence for an active role of microtubules in cytoplasmic transport. *J. Cell Biol*. **100**, 1736-1752.

Atkinson, S. J., Doberstein, S. K. and Pollard, T. D. (1992). Axonal transport moving off the beaten track. *Curr. Biol.* **2**, 326-328.

Benashski, S. E., Harrison, A., Patel-King, R. S. and King, S. M. (1997). Dimerization of the highly conserved light chain shared by dynein and myosin V. *J. Biol. Chem*. **272**, 20929-20935.

Bobola, N., Jansen, R. P., Shin, T. H. and Nasmyth, K. (1996) Asymmetric accumulation of Ash1p in postanaphase nuclei depends on a myosin and restricts yeast mating-type switching to mother cells. *Cell* **84**, 699-709.

Brady, S. T., Pfister, K. K. and Bloom, G. S. (1990). A monoclonal antibody against kinesin inhibits both anterograde and retrograde fast axonal transport in squid axoplasm. *Proc. Nat. Acad. Sci. USA* **87**, 1061-1065.

Cheney, R. E. and Mooseker, M. S. (1992). Unconventional myosins. *Curr. Opin. Cell Biol.* **4**, 27-35.

Cheney, R. E., O'Shea, M. K., Heuser, J. E., Coelho, M. V., Wolenski, J. S., Espreafico, E. M., Forscher, P., Larson, R. E. and Mooseker, M. S. (1993a). Brain myosin-V is a two-headed unconventional myosin with motor activity. *Cell* **75**, 13-23.

Cheney, R. E., Riley, M. A. and Mooseker, M. S. (1993b). Phylogenetic analysis of the myosin superfamily. *Cell Motil. Cytoskel.* **24**, 215-223.

Cohen, D. L., Kuznetsov, S. A. and Langford, G. M. (1994). Myosin V in squid axoplasm and optic lobes. *Mol. Biol. Cell* **5**, 278A.

Dekker-Ohno, K., Hayasaka, S., Takagishi, Y., Oda S., Wakasugi, N., Mikoshiba, K., Inouye, M. and Yamamura, H. (1996). Endoplasmic reticulum is missing in dendritic spines of Purkinje cells of the ataxic mutant rat. *Brain Res.* **714**, 226-230.

Ellisman, M. H. and Lindsey, J. D. (1983). The axoplasmic reticulum within myelinated axons is not transported rapidly. *Neurocytol* **12**, 393-411.

Erdelyi, M., Michon, A. M., Guichet, A., Glotzer, J. B. and Ephrussi, A. (1995). Requirement for Drosophila cytoplasmic tropomyosin in oskar mRNA localization. *Nature* **377**, 524-527.

Espindola, F. S., Espreafico, E. M., Coelho, M. V., Martins, A. R., Costa, F. R., Mooseker, M. S. and Larson, R. E. (1992). Biochemical and immunological characterization of p190-calmodulin complex from vertebrate brain: a novel calmodulin-binding myosin. *J. Cell Biol.* **118**, 359-368.

Espindola, F. S., Cheney, R. E., King, S. M., Suter, D. M. and Mooseker, M. S. (1996). Myosin-V and dynein share a similar light chain. *Mol. Biol. Cell* **7**, 372a.

Espreafico, E. M., Cheney, R. E., Matteoli, M., Nascimento, A. A., De Camilli, P. V., Larson, R. E. and Mooseker, M. S. (1992). Primary structure and cellular localization of chicken brain myosin-V (p190), an unconventional myosin with calmodulin light chains. *J Cell Biol*. **119**, 1541-1557.

Evans, L. L., Hammer, J. and Bridgman, P. C. (1997). Subcellular localization of myosin V in nerve growth cones and outgrowth from dilute-lethal neurons. *J. Cell Sci.* **110**, 439-449.

Evans, L. L., Lee, A. J., Bridgemen, P. C. and Mooseker, M. S. (1998). Vesicle-associated brain myosin-V can be activated to catalyze actin-based transport. *J. Cell Sci.* **111**, 2055-2066.

Gilbert, S. P., Webb, M. R., Brune, M. and Johnson, K. A. (1995). Pathway of processive ATP hydrolysis by kinesin. *Nature* **373**, 671-676.

Govindan, B., Bowser, R. and Novick, P. (1995). The role of Myo2, a yeast class V myosin, in vesicular transport. *J. Cell Biol.* **128**, 1055-1068.

Haarer, B. K., Petzold, A., Lillie, S. H. and Brown, S. S. (1994). Identification of MYO4, a second class V myosin gene in yeast. *J. Cell Sci*. **107**, 1055-1064.

Hackney, D. D. (1995). Highly processive microtubule-stimulated ATP hydrolysis by dimeric kinesin head domains. *Nature* **377**, 448-450.

Hill, K. L., Catlett, N. L. and Weisman, L. S. (1996). Actin and myosin function in directed vacuole movement during cell division in Saccharomyces cerevisiae. *J. Cell Biol*. **135**, 1535-1549.

Hodge, A. J. and Adelman, W. J. Jr (1980). The neuroplasmic network in Loligo and Hermissenda neurons. *J. Ultrastruct. Res.* **70**, 220-241.

Howard, J. (1997). Molecular motors: structural adaptations to cellular functions. *Nature* **389**, 561-567.

Hurvitz, H., Gillis, R., Klaus, S., Klar, A., Gross-Kieselstein, F. and Okon, E. (1993). A kindred with Griscelli disease: spectrum of neurological involvement. *Eur. J. Pediatr.* **152**, 402-405.

Johnston, G. C., Prendergast, J. A. and Singer, R. A. (1991). The Saccharomyces cerevisiae MYO2 gene encodes an essential myosin for vectorial transport of vesicles. *J. Cell Biol.* **113**, 539-551.

Kuznetsov, S. A., Langford, G. M. and Weiss, D. G. (1992). Actin-dependent organelle movement in squid axoplasm. *Nature* **356**, 722-725.

Kuznetsov, S. A., Rivera, D. T., Severin, F. F., Weiss, D. G. and Langford, G. M. (1994). Movement of axoplasmic organelles on actin filaments from skeletal muscle. *Cell Motil. Cytoskel*. **28**, 231-242.

Laemmli, U. K. (1970). Cleavage of structural proteins during the assembly of the head of bacteriophage T4. *Nature* **227**, 680-685.

Langford, G. M., Kuznetsov, S. A., Johnson, D., Cohen, D. L. and Weiss, D. G. (1994). Movement of axoplasmic organelles on actin filaments assembled on acrosomal processes: evidence for a barbed-end-directed organelle motor. *J. Cell Sci.* **107**, 2291-2298.

Langford, G. M. (1995). Actin- and microtubule-dependent organelle motors: interrelationships between the two motility systems. *Curr. Opin. Cell Biol.* **7**, 82-88.

Langford, G. M. and Molyneaux, B. J. (1998). Myosin V in the brain: mutations lead to neurological defects. *Brain Res. Rev.* (in press).

Larson, R. E. (1996). Myosin-V: a class of unconventional molecular motors. *Braz. J. Med. Biol. Res.* **29**, 309-318.

Leopold, P. L., McDowall, A. W., Pfister, K. K., Bloom, G. S. and Brady,

S. T. (1992). Association of kinesin with characterized membrane-bounded organelles. *Cell Motil. Cytoskel.* **23**, 19-33.

Long, R. M., Singer, R. H., Meng, X., Gonzalez, I., Nasmyth, K. and Jansen, R. P. (1997). Mating type switching in yeast controlled by asymmetric localization of ASH1 mRNA. *Science* **277**, 383-387.

Lucero, H. A, Lebeche, D. and Kaminer, B. (1994). ERcalcistorin/protein disulfide isomerase (PDI). Sequence determination and expression of a cDNA clone encoding a calcium storage protein with PDI activity from endoplasmic reticulum of the sea urchin egg. *J. Biol. Chem.* **269**, 23112-23119.

Lucero, H. A., Lebeche, D. and Kaminer, B. (1998). ERcalcistorin/protein disulfide isomerase acts as a calcium storage protein in the endoplasmic reticulum of a living cell. *J. Biol. Chem.* **273**, 9857-9863.

Mage, M. G. (1980). Preparation of Fab fragments from IgGs of different animal species. *Meth. Enzymol.* **70**, 142-150**.**

Mercer, J. A., Seperack, P. K., Strobel, M. C., Copeland, N. G. and Jenkins, N. A. (1991). Novel myosin heavy chain encoded by murine dilute coat color locus. *Nature* **349**, 709-713.

Mermall, V., Post, P. L. and Mooseker, M. S. (1998). Unconventional myosins in cell movement, membrane traffic, and signal transduction. *Science* **279**, 527-533.

Metuzals, J., Hodge, A. J,. Lasek, R. J. and Kaiserman-Abramof, I. R. (1983). Neurofilamentous network and filamenouus matrix preserved and isolated by different techniques from squid giant axon. *Cell Tissue Res*. **228**, 415-432.

Metuzals, J., Chang, D., Hammar, K. and Reese, T. S. (1997). Organization of the cortical endoplasmic reticulum in the squid giant axon. *J. Neurocytol*. **26**, 529-539.

Mooseker, M. S. and Cheney, R. E. (1995). Unconventional myosins. *Annu. Rev. Cell Dev. Biol.* **11**, 633-675.

Molyneaux, B. J. and Langford, G. M. (1997). Characterization of antibodies to the head and tail domains of squid brain myosin V. *Biol. Bull*. **193**, 222-223.

Moritz, R. L., Eddes, J., Hong, J., Reid, G. E. and Simpson, R. J. (1995). Rapid separation of proteins and peptides using conventional silica-based supports: identification of 2-D gel proteins following in-gel proteolysis. In *Techniques in Protein Chemistry VI* (ed. J. W. Crabb), pp 311-319. Academic Press, San Diego.

Morris, J. R. and Lasek, R. J. (1982). Stable polymers of the axonal cytoskeleton: the axoplasmic ghost. *J. Cell Biol.* **92**, 192-198.

Morris, J. R. and Lasek, R. J. (1984). Monomer-polymer equilibria in the axon: direct measurement of tubulin and actin as polymer and monomer in axoplasm. *J. Cell Biol.* **98**, 2064-2076.

Nakata, T., Terada, S. and Hirokawa, N. (1998). Visualization of the dynamics of synaptic vesicle and plasma membrane proteins in living axons. *J. Cell Biol.* **140**, 659-674.

Nascimento, A. A. C., Cheney, R. E., Tauhata, S. B. F., Larson, R. E. and Mooseker, M. S. (1996). Enzymatic characterization and functional domain mapping of brain myosin-V. *J. Biol. Chem*. **271**, 17561-17569.

Nascimento, A. A. C., Amaral, R. G., Bizario, J. C. S., Larson, R. E. and Espreafico, E. M. (1997). Subcellular localization of myosin-V in the B16 melanoma cells, a wild-type cell line fron the dilute gene. *Mol. Biol. Cell* **8**, 1971-1978.

Ostap, E. M. and Pollard, T. D. (1996). Overlapping functions of myosin-I isoforms? *J. Cell Biol*. **133**, 221-224.

Pardee, J. D. and Spudich, J. A. (1982). Mechanism of K+-induced actin assembly. *J. Cell Biol*. **93**, 648-654.

Ponting, C. P. (1995). AF-6/cno: neither a kinesin nor a myosin, but a bit of both. *Trends Biochem. Sci*. **20**, 265-266**.**

Pastural, E., Barrat, F. J., Dufourcq-Lagelouse, R., Certain, S., Sanal, O., Jabado, N., Seger, R., Griscelli, C., Fischer, A. and de Saint Basile, G. (1997). Griscelli disease maps to chromosome 15q21 and is associated with mutations in the myosin-Va gene. *Nature Genet.* **16**, 289-292.

Prekeris, R. and Terrian, D. M. (1997). Brain myosin V is a synaptic vesicle-associated motor protein: evidence for a Ca^{2+}-dependent interaction with the synaptobrevin-synaptophysin complex. *J. Cell Biol*. **137**, 1589-1601.

Provance, D. W. Jr, Wei, M., Ipe, V. and Mercer, J. A. (1996). Cultured melanocytes from dilute mutant mice exhibit dendritic morphology and altered melanosome distribution. *Proc. Nat. Acad. Sci. USA* **93**, 14554-14558.

Santos, B. and Snyder, M. (1997). Targeting of chitin synthase 3 to polarized growth sites in yeast requires Chs5p and Myo2p. *J. Cell Biol*. **136**, 95-110.

Sitia, R. and Meldolesi, J. (1992). Endolasmic reticulum: a dynamic patchwork of specialized subregions. *Mol. Biol. Cell* **3**, 1067-1072.

Steffen, W., Hodgkinson, J. L. and Wiche, G. (1996). Immunogold localization of the intermediate chain within the protein complex of cytoplasmic dynein. *J. Struct. Biol.* **117**, 227-235.

Tabb, J. S., Harmon, K. O., DePina, A. S. and Langford, G. M. (1996). Localization of myosin on tubulovesicular organelles in the squid giant axon by immuno-EM. *Biol. Bull.* **191**, 274-275.

Takagishi, Y., Oda, S., Hayasaka, S., Dekker-Ohno, K., Shikata, T., Inouye, M. and Yamamura, H. (1997). The dilute-lethal (dl) gene attacks a Ca^{2+} store in the dendritic spine of Purkinje cells in mice. *Neurosci. Lett.* **215**, 169-172.

Takizawa, P. A., Sil, A., Swedlow, J. R., Herskowitz, I. and Vale, R. D. (1997). Actin-dependent localization of an RNA encoding a cell-fate determinant in yeast. *Nature* **389**, 90-93.

Terasaki, M. and Jaffe, L. A. (1993). Imaging endoplasmic reticulum in living sea urchin eggs. *Meth. Cell Biol.* **38**, 211-220.

Terasaki, M., Song, J., Wong, J. R., Weiss, M. J. and Chen, L. B. (1984). Localization of endoplasmic reticulum in living and glutaraldehyde-fixed cells with fluorescent dyes. *Cell* **38**, 101-108.

Titus, M. A. (1997). Unconventional myosins: new frontiers in actin-based motors. *Trends Cell Biol.* **7**, 119-123.

Tsukita, S. and Ishikawa, H. (1980). The movement of membranous organelles in axons. Electron microscopic identification of anterogradely and retrogradely transported organelles. *J.Cell Biol* **84,** 513-530.

Vale, R. D., Fanatsu, T., Pierce, D. W., Romberg, L., Harada, Y. and Yanagida, T. (1996). Direct observation of single kinesin molecules moving along microtubules. *Nature* **380**, 451-453.

Vale, R. D. (1996). Switches, latches, and amplifiers: common themes of G proteins and molecular motors. *J. Cell Biol.* **135**, 291-302.

Walch-Solimena, C., Collins, R. N. and Novick, P. J. (1997). Sec2p mediates nucleotide exchange on Sec4p and is involved in polarized delivery of post-Golgi vesicles. *J. Cell Biol*. **137**, 1495-1509.

Wang, F. S., Wolenski, J. S., Cheney, R. E., Mooseker, M. S. and Jay, D. G. (1996). Function of myosin-V in filopodial extension of neuronal growth cones. *Science* **273**, 660-663.

Weiss, D. G., Langford, G. M., Seitz-Tutter, D., Gulden, J. and Keller, F. (1988). Motion analysis of organelle movements and microtubule dynamics. In *Structure and Functions of the Cytoskeleton. La Structure et Les Fonctions du Cytosquelette. Biological and physiopathological Aspects*. Colloque INSERM vol. 171 (ed. B. Rousset). INSERM-John Libbey Eurotext, Paris/London, 15 s., im Druck.

Weiss, D. G., Maile, W. and Wick, R. A. (1989). Video microscopy. In *Electronic Light Microscopy in Biology - A Practical Approach* (ed. A. J Lacey), pp. 221-278. IRL Press, Oxford.

Wolenski, J. S., Cheney, R. E., Forscher, P. and Mooseker, M. S. (1993). In vitro motilities of the unconventional myosins, brush border myosin-I, and chick brain myosin-V exhibit assay-dependent differences in velocity. *J. Exp. Zool*. **267**, 33-39.

Wolenski, J. S., Cheney, R. E., Mooseker, M. S. and Forscher, P. (1995). In vitro motility of immunoadsorbed brain myosin-V using a Limulus acrosomal process and optical tweezer-based assay. *J. Cell Sci*. **108**, 1489-1496.

Wu, X., Bowers, B., Wei, Q., Kocher, B. and Hammer, J. A. 3rd (1997). Myosin V associates with melanosomes in mouse melanocytes: evidence that myosin V is an organelle motor. *J. Cell Sci.* **110**, 847-859.